Augmentation of Class-E PA reliability under load mismatch conditions

Jeroen Ponte

Supervisor:

MSc. A. Ghahremani

Committee:

MSc. A. Ghahremani

Prof.dr.ir. A.J. Annema

Prof.dr.ir. L.J. Spreeuwers

Abstract

Class-E PAs present significant efficiency advantages over other PA topologies, but are sensitive to load mismatch. Extreme cases of load mismatch can lead to reliability issues.

In this work, a system for automatically compensating for load variations in Class E PAs, to increase reliability aspects, was developed. This work extends current research work by Ali Ghahremani.

A proof of concept demonstrator was built, using class-E PA chips that were previously designed in the SHERPAS research project. To confirm the theory, a measurement setup was developed where load mismatch was reliably set using a PC-controlled antenna tuner setup. A PC-connected oscilloscope, with an active differential probe, was be used to sense the peak drain voltage of the PA. The obtained information was be processed by PC software (e.g. MATLAB) to predict the amount of additional switch parallel capacitance required to compensate the PA to operate under the present load mismatch. A PC-controlled microcontroller allows capacitors aboard the Class E PA integrated circuit to be switched in or out, providing improved load matching.

The results show increased safe area on the Smith chart as well as improved efficiency, providing strong confidence in the validity of the theoretical work by Ali Ghahremani.

Contents

1 Introduction

RF power amplifiers (PAs) are an essential building block in modern wireless communication systems. Because the PA's power consumption generally represents a significant portion of total system power consumption, its efficiency is an important parameter, especially in battery-powered equipment.

PAs operating in Class E present distinct efficiency advantages over other amplifier classes, with 100% efficiency theoretically attainable with ideal components [3]. However, due to their tuned nature, Class-E PA behavior is strongly influenced by variations in load impedance [1].

Because the antenna impedance can generally not be well-controlled, especially in portable applications, either a variable tuning network to match the antenna to the PA or variable tuning of the PA itself is required to avoid conditions with severe efficiency and reliability penalties.

In previous work [2], extensive Class-E PA theory was developed. This was extended in [1] to investigate the possibility of (re-)tuning Class-E PAs to enhance their reliability. In this work, the application of this tuning is explored and experiments are performed to confirm its validity.

1.1 Goals

The goal of this assignment is to develop an automatic PA-compensating system that actively monitors and adjusts the behavior of a Class-E PA through tuning. This is a valuable endeavor because it accommodates increased reliability and efficiency, allowing more effective application of Class-E PAs in situations where strong load variations may occur. The applied compensation is based on extensive theoretical and practical work performed in [1], which is explored and applied in this work to illustrate the effects of the automatic tuning system on PA behavior.

Measurements will be done on the resulting system to confirm its functionality. Finally, the implications will be discussed and suggestions for future work will be made.

2 Class-E PAs

In this section, the concept Class-E PAs is introduced. Some intuitive analysis is performed on Class-E PA models with varying levels of simplification and the PA parameters and their influences are discussed.

2.1 Basics of Class-E PAs

Class-E PAs are a class of switching PAs. In a single-ended configuration, as treated in this work, they consist of a switch and two tuned networks, one of which is the switch parallel tank and the other the series load tank. The parallel network allows for ideally lossless energy storage while the series tank filters the switch voltage waveform so that ideally energy is only transferred at the fundamental of the driving frequency. The latter is important because the intention is to transmit at the fundamental frequency: any overtone energy into the load is effectively wasted and, in severe cases, may break transmission regulations. It is for this reason that the efficiency of the PA is defined for the fundamental power into the load rather than the total power.

A schematic representation of a single-ended Class-E PA (henceforth referred to as *Class-E PA*) can be seen in Figure 1.

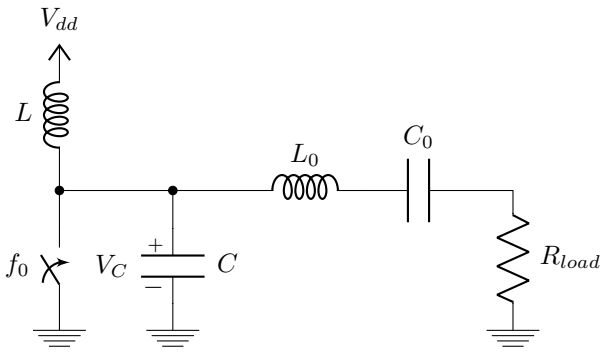

Figure 1: Schematic representation of a single-ended Class-E PA

2.2 Principle of operation

To investigate the principle of operation of the Class-E PA, some simplified versions of the circuit are considered first. An ideal switch and ideal components are assumed, unless mentioned otherwise.

2.2.1 Unloaded case with single switching moment

When the switch is closed at $t = 0$ until $t = t_0$ and then opened and left open, an undamped oscillation (around the steady-state point of V_{dd}) can be seen on the switch parallel capacitor. A schematic representation of the circuit is shown in Figure 2.

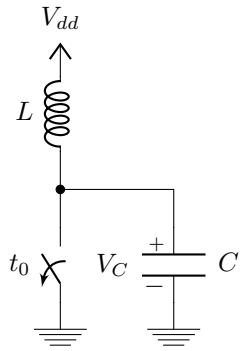

Figure 2: Schematic representation of unloaded single switching moment case, t_0 represents the moment the switch is opened

The energy in the system (assuming zero initial energy - $I_L(0) = 0A$) is given by the energy transferred into inductor while the switch is closed as-

$$E_L = \frac{I^2 L}{2} = \frac{\left(\frac{V_{dd}}{L} t_0\right)^2 L}{2} = \frac{\left(\frac{V_{dd}}{\sqrt{L}} t_0\right)^2}{2} \tag{1}$$

It can be shown that the time-dependent capacitor voltage behavior after the switch is opened is given by-

$$V_C(t) = V_{dd} + \frac{V_{dd} T_{on}}{\sqrt{LC}} sin\left(\frac{1}{\sqrt{LC}}(t - t_0)\right) = V_{dd} + \sqrt{\frac{2E_L}{C}} sin\left(\frac{1}{\sqrt{LC}}(t - t_0)\right), \quad t \geq t_0 \tag{2}$$

This shows that the oscillation amplitude is dependent on the inductor energy and the parallel switch capacitance.

2.2.2 Unloaded case with periodic switching

The schematic representation is the same as given in Figure 2 but with periodic switching at frequency f_0.

When the switch is periodically cycled with an on-time of T_{on}, energy is continually added to the inductor. Additionally, when the switch is turned on at a moment where the capacitor voltage is non-zero, energy is lost as given by-

$$E_{loss} = \frac{CV^2(t_{on}^-)}{2} \tag{3}$$

Where t_{on}^- is the moment right before the switch is closed.

The energy added to the inductor is also dependent on the current at the switch turn-on moment by-

$$E_L = \frac{\left(\frac{V_{dd}}{L}T_{on} + I_L(t_{on}^-)\right)^2 L}{2} \tag{4}$$

Giving an extra non-constant added energy per cycle of-

$$\Delta E_L = I_L(t_{on}^-)V_{dd}T_{on} + \frac{I_L^2(t_{on}^-)L}{2} \tag{5}$$

The interplay of these energies gives rise to somewhat complex behavior. However, some conclusions can still be drawn.

The balance between energy added to the inductor during, and removed from the capacitor at, the switch-on moment determines the capacitor voltage. Shifting this balance changes the circuit behavior by varying the average system energy. High energy gives rise to high maximum capacitor voltages and vice versa, so energy should be kept low to avoid extreme maximum switch voltages.

It can be seen that changing the parallel tank resonant frequency alters the voltage waveform phase at the switching moment. This relates directly to the switching energy loss by a change of the capacitor voltage at the switch turn-on moment. It should be noted that this also proportionally changes the oscillation amplitude, indirectly for the inductor through the inductor energy and directly for the capacitor.

Similarly, the energy loss per cycle can also be changed by modifying the switching moment along the voltage waveform, while simultaneously affecting the inductor energy added each cycle.

Some waveforms to illustrate the discussed influences are shown in Figure 3

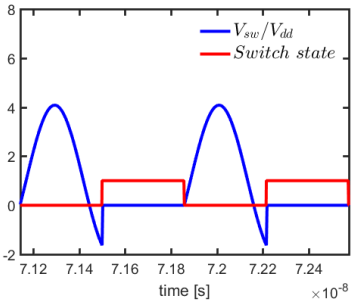

(a) q=1.412 and d=1

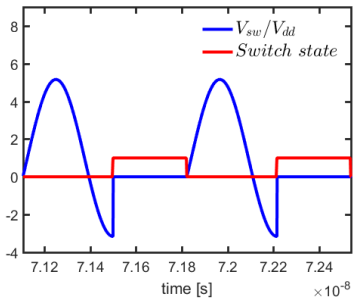

(b) q=1.412 and d=0.9

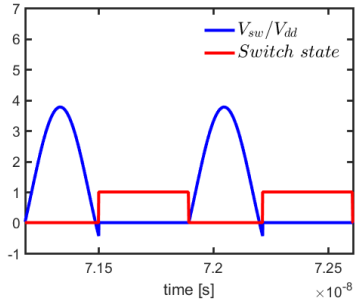

(c) q=1.412 and d=1.1

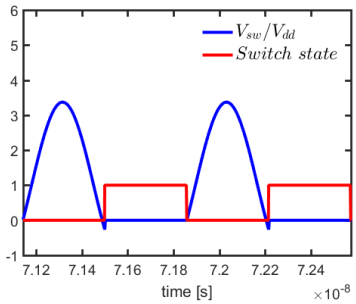

(d) q=1.3 and d=1

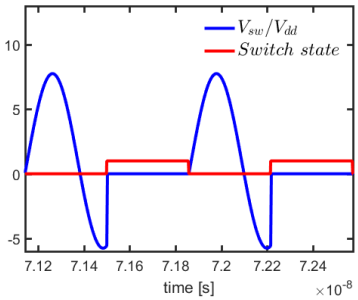

(e) q=1.6 and d=1

Figure 3: The behavior of an unloaded Class-E PA with nominal design q=1.412 and d=1 for varying d and q

2.2.3 Loaded case with periodic switching

When the tuned load is introduced, the circuit behavior is further complicated. This is caused by the addition or removal of current to the capacitor by the load and the complicated start-up behavior. The former heavily modifies the

oscillation waveform while the latter complicates intuitive analysis. The interaction between the load and switch tank allow the waveform to be shaped such that zero voltage and zero slope can be achieved at the switching moment (ZVS and ZSS). ZVS conditions allow (ideally) zero switching loss and ZSS conditions minimize energy loss due to the switch transitioning through its linear region by keeping the voltage low around the switching moment.

2.2.4 Some influences of non-ideal components

Previously, ideal components were considered. Here, some effects of the more prominent component non-idealities are treated.

A non-ideal switch with finite on-resistance predominantly influences the energy loss during the switch on-time and the added and maximum inductor energy by limiting the steady-state on-current. Additionally, it complicates the switch voltage behavior during on-time by not clamping it to $0V$ during the switch on-state.

Similarly, a non ideal inductor with finite equivalent series resistance (ESR) causes energy losses and limits steady-state on-current, together with the switch to $\frac{V_{dd}}{R_{on}+R_{ESR}}$.

Capacitor ESR also causes resistive losses, but these are normally less significant as the capacitor current is ideally harmonic only. Also, capacitor ESR tends to be lower than inductor ESR.

A limited-Q load tank gives rise to energy loss at harmonic overtones, which relates to some extent to finite ESR in the load tank capacitor and inductor, which by themselves cause energy loss at the fundamental, as well. Additionally, the assumption of a sinusoidal load current made in [1] and [2] will be violated.

2.3 Class-E subclasses

In [2], three subclasses of Class-E PAs are identified for the behavior of the switch voltage waveform at the switching moment. For the so-called optimum Class-E PA, the switch voltage reaches both ZVS and ZSS at the switching moment. The former is related to efficiency because when switching at non-zero voltage energy is lost as was given by Equation 3.

When this discharging occurs every switching moment, the energy loss is periodic and can be expressed as power dissipation by-

$$P_{diss} = \frac{CV^2\left(t^-_{switch}\right)}{2} f_0 = \frac{CV^2\left(t^-_{switch}\right)}{4\pi} \omega_0 \tag{6}$$

The (level of) violation of ZVS and ZSS conditions are expressed in the parameters α and β, respectively, as follows-

$$V_C\left(\frac{2\pi}{\omega_0}\right) = \alpha V_{dd} \tag{7}$$

$$\frac{dV_C}{dt}\left(\frac{2\pi}{\omega_0}\right) = \beta\omega_0 V_{dd} \tag{8}$$

When ZVS conditions are violated while ZSS conditions are maintained, the resulting Class-E PA is labeled as a variable-voltage Class-E, or Class-E_{VV} for short. The voltage level at the switching moment normalized to V_{dd} is expressed as α.

Alternatively, when ZSS conditions are violated while ZVS conditions are maintained, the resulting Class-E PA is known as a variable-slope Class-E, or Class-E_{VS} for short. The slope level at the switching moment normalized to $\omega_0 V_{dd}$ is expressed in parameter as β.

This work is concerned only with the optimal Class-E. However, some of the discussed concepts can be extended to the other subclasses.

2.4 K-design set

In [2], Class-E PA behavior was examined mathematically and a design procedure was formulated using a set of developed relations named the K-design set. Values for the K set are found using a curve fit to allow easier computation. The values in the design set are non-linearly dependent on PA parameters d, q and m, which are the switching duty cycle, relative resonance frequency and switch on resistance, respectively, given as-

$$S \triangleq \begin{cases} on; & 0 < \omega_0 t < d\pi \\ off; & d\pi < \omega_0 t < 2d\pi \end{cases} \tag{9}$$

$$q = \frac{1}{\omega_0\sqrt{LC}} \tag{10}$$

$$m = \omega_0 R_{on} C \tag{11}$$

The K-design set is shown in Table 1.

Table 1: K-Design set

$K_L = \frac{L\omega_0}{R}$	$K_C = \omega_0 RC$	$K_X = \frac{X}{R}$	$K_P = \frac{RP_{out}}{V_{dd}^2}$

2.5 Load mismatch

Because Class-E PAs employ tuned networks, their behavior is heavily influenced by load conditions. Deviations from nominal (i.e. designed-for) load conditions cause degradation in efficiency and, more problematically, variation in maximum and minimum switch voltage and current. Large switch voltage can cause breakdown events while large currents can cause thermal destruction, both of which potentially damaging or destroying the switch, rendering the PA inoperable. Reliability was discussed in more detail in [2].

3 Class-E PA load effects

In this section, the effects of load variation on Class-E PAs is investigated further. The main parameters of interest are maximum switch voltage, maximum switch current and PA efficiency. The latter is defined as switch efficiency as-

$$\eta = \frac{P_{DC}}{P_{load}}$$

This efficiency differs from power added efficiency (PAE) in that the power required to drive the switch is not taken into account.

The behavior of the Class-E PA is quite complex due to the combination of two tuned tanks and the non-linear switching behavior. For this reason, the PA behavior is investigated mathematically using the equations developed in [1]. The results are presented in the form of contour plots to give a concise and clear overview. The Smith chart is used to graphically present PA behavior, as it contains all possible positive magnitude load impedances.

3.1 Contour plots

The PA investigated in this work was designed for $q = 1.412$, $d = 1$, $m = 0.05$ and $V_{dd} = 1.2V$. Nominal switch voltage and efficiency data for a load varying across the Smith chart is shown in Figure 4.

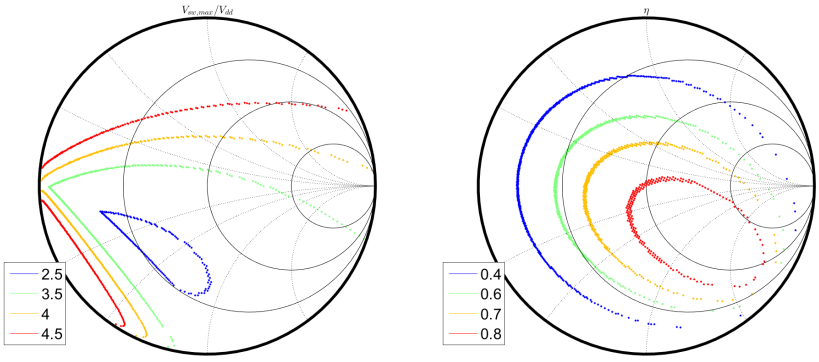

(a) Maximum switch voltage contours (b) Efficiency contours

Figure 4: Class-E PA contours for $q_{nom} = 1.412$, $d_{nom} = 1$ and $m = 0.05$

It can be seen that a portion of the Smith chart shows sub-nominal (safe) behavior. This shows that the PA reliability is only degraded in part of the Smith chart. If the safe zone can be extended by tuning, the PA can be made more rugged. The efficiency for nominal load can be seen to be part of a contour,

i.e. high efficiency can be obtained for different loads on the contour. The degradation of efficiency follows a similar trend to the increase of the maximum switch voltage.

4 Tuning methods

It was shown, using the Smith chart, that load variations strongly affect Class-E PA behavior. To regain nominal or near-nominal behavior, the PA or load must be (re-)tuned. This can be done in several ways, some more practical than others.

In this section, different methods of tuning and their advantages and disadvantages are discussed. Finally, a tuning method is chosen and its consequences on PA behavior is shown graphically. Lastly a method for tuning the PA using the chosen method is treated.

4.1 Load tuning

One available option is to tune the load back to nominal conditions. This can be done by means of a controlled matching network. Higher levels of complexity could increase the tuning range of the network, allowing it to cover a large portion of the Smith chart.

A major drawback of this type of tuning is present in the fact that a different type of network is required for different points on the Smith chart. Points on the resistive line require pure voltage scaling (i.e. using a transformer), while points of complex impedance require a complex compensating impedance (i.e. shunt and series capacitance or series inductance and capacitance).

These previous points imply the need for a complicated and extensive tuning network, increasing chip size. Besides this, the network would be complicated to properly analyze and design and therefore be highly impractical.

4.2 PA tuning

An alternative option is present in tuning of the PA itself by changing either or both the d and q parameters. Changing the drive frequency would also allow some tuning of PA behavior but this is generally undesirable because the receiver would have to track the variation in frequency.

The q parameter can be tuned independently of the load by variations in either or both the parallel switch inductor and capacitor. Because inductors would imply a scheme where the R_{on} of the switches add (e.g. a series string of selectively short-circuited inductors), while for switched capacitance they are in parallel (with a ratio due to the capacitor ratio), capacitance variation presents the superior choice for tuning q. The concept of the implementation used in [1] and this work is shown schematically in Figure 5

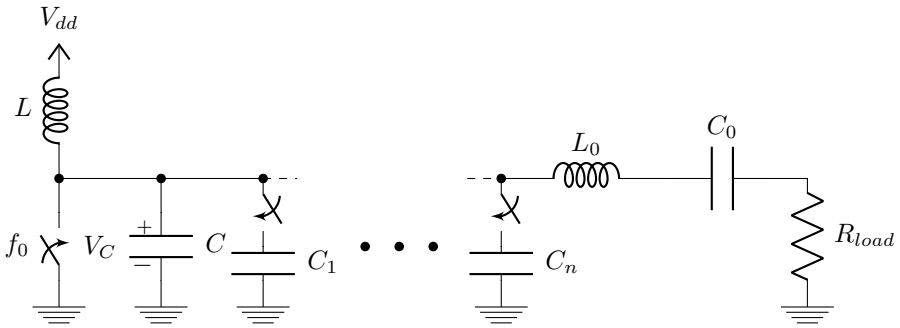

Figure 5: Schematic representation of single-ended Class-E PA with capacitor bank for tuning of the q parameter

The d parameter can be tuned by modifying the switching point. This can be achieved by e.g. driving a high gain switch driver with a non-square wave (e.g. a sinusoid or triangle waveform) and adding a DC offset to shift the switch trigger level along the input waveform.

A potential downside of tuning with the d parameter is that the drive power stays roughly constant while the load power changes, leading to degradation in PAE for lower load power.

4.3 Tuning of the q parameter

When changing the parallel switch capacitance such that the q parameter is lowered from the nominal condition, $q = 1.412$, to the new condition, $q = 1.172$, the maximum switch voltage and efficiency contour plots in Figure 6 result.

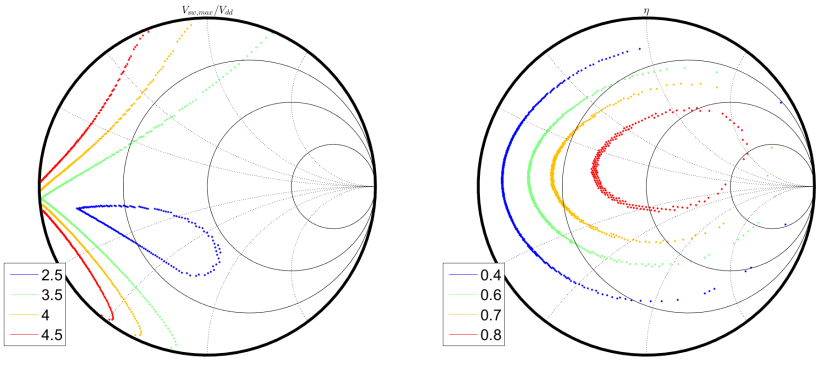

(a) Maximum switch voltage contours (b) Efficiency contours

Figure 6: Class-E PA contours for $q_{nom} = 1.412$, $d_{nom} = 1$, $m = 0.05$ and $q_{new} = 1.172$

It can be seen that the extreme voltage and current behavior contours have

'migrated' towards the lefthand extreme ($R = 0\Omega$) of the Smith chart when compared to Figure 4, while the efficiency contours have rotated. The portion of the Smith chart with nominal and sub-nominal maximum switch voltage behavior has increased.

The safe area of the PA has increased, showing that the PA is capable of withstanding more extreme load mismatch in the tuned case than the nominal case. Additionally, the extremity of the worst case behavior has also reduced.

4.4 Automatic PA tuning

To allow the PA to perform more optimally under a variety of load conditions, dynamic tuning can be applied. As can be seen from the previously shown contours, this offers efficiency advantages over setting the capacitor bank statically to its maximum capacitance.

Because the main goal of the tuning system in this work is to keep the PA from operating in an area of reduced reliability, a simple implementation can be made by measuring the switch peak voltage and keeping it below a set limit by tuning the capacitor bank. To take advantage of the efficiency benefits, the system should constantly re-tune the PA to maintain conditions as close as possible to optimum. The easiest way to achieve this explicitly is by means of an under-over algorithm that tunes the PA by finding the capacitor bank state where the PA operates minimally below the switch voltage limit. To ensure the PA is adjusted quickly when a severe violation of the maximum switch voltage occurs, a trip limit is implemented beyond which the entire capacitor bank is switched in.

A flow diagram of the self-healing algorithm can be found in Figure 7.

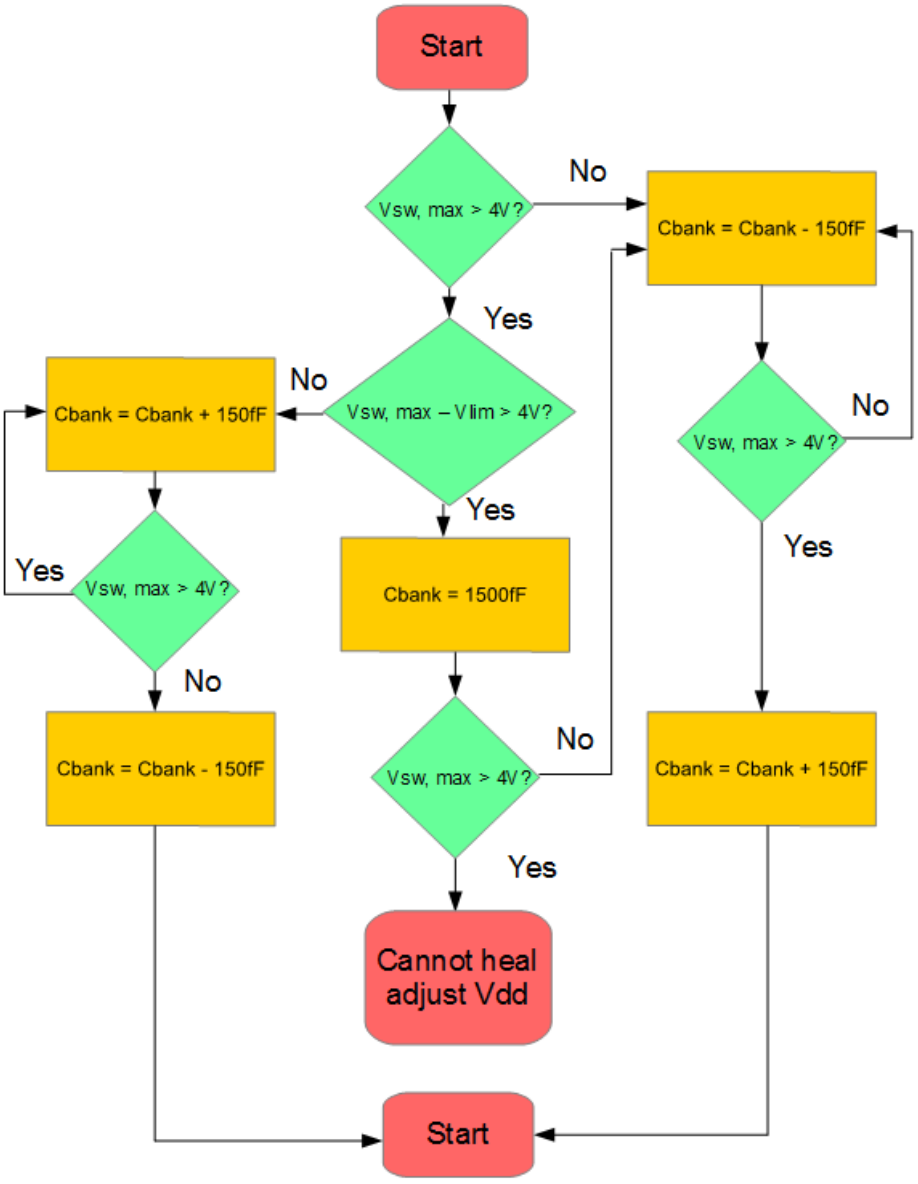

Figure 7: Self-healing algorithm flow diagram

4.5 Peak detection

To produce a standalone version of the PA tuning system, the switch peak voltage should be detected. It can then be digitized using an A-to-D converter and processed using a tuning algorithm running on a capable micro-controller.

The simplest implementation of a peak detector is found in the use of a diode with hold capacitor. To work effectively, this diode should have as little parasitic capacitance and inductance as possible, the former for isolation and the latter for transient response. With this implementation, an issue presents itself in that an idealized version of the circuit (i.e. no voltage droop) stores the highest value in its history. As such, it does not allow for checking a local maxima, meaning a lower peak voltage after tuning cannot be detected.

To counteract this problem, the capacitor voltage can be gradually decreased by means of a parallel current sink or resistor. This, however, causes an error dependent on the readout frequency, detector output level, and capacitor and current or resistor value.

A more convenient solution can be found in the use of a reset switch that resets the storage capacitor, allowing algorithmic control of the window in which a maximum is to be read while possessing minimal droop if well designed. To avoid loading of the PA, the peak detector can be switched out of circuit during the reset pulse, or a resistor can be introduced between the diode cathode and storage capacitor. The latter introduces a time-constant and possible parasitic inductance, so the former is preferred. A dead time (i.e. time between the opening of the diode switch and closing of the hold capacitor switch) can be introduced to avoid problems due to timing errors and switch transients but this is not further discussed here.

Care must be taken in the selection of the hold capacitor value. A large capacitor would cost significant energy to be charged to its final value, while the use of a small capacitor leads to more sensitivity to leakage currents. Additionally, the discharging of the hold capacitor may generate electromagnetic interference if it is not performed carefully.

A schematic representation and simulation of the final concept are shown in Figure 8 and 9, respectively. A simulation of the circuit was performed in LTspice XVII, with a model of the BAT62-L704 supplied by Infineon used for the diode.

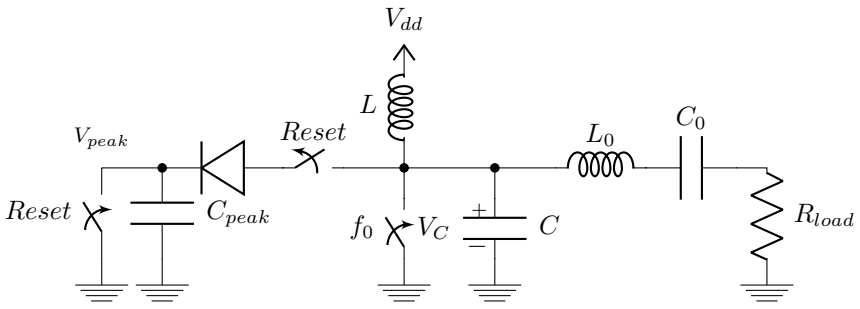

Figure 8: Schematic representation of single-ended Class-E PA with peak detector

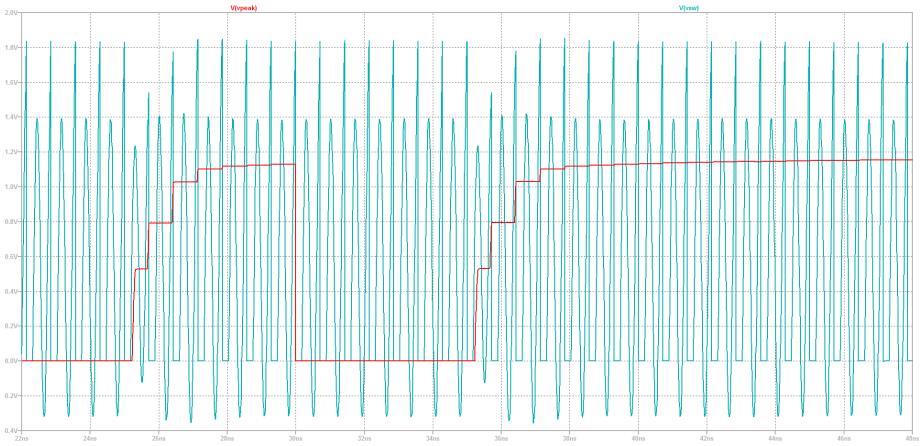

Figure 9: Peak detector and PA switch voltage waveforms

The difference between the actual peak value and the peak detector output value is due to the diode forward voltage drop. This drop can be measured and calibrated out, leaving the diode forward voltage temperature coefficient and drift as the main remaining sources of error. If the temperature drift is too significant, the forward voltage can be calibrated at different temperatures. Then, using a temperature sensor, the temperature calibration data can be interpolated to produce (some degree of) cancellation of the detector error at any operating temperature.

A change in the switch voltage waveform can be seen at the reset moment due to the current transient caused by the absence of dead-time. This will lead to power loss and create undesirable transients in the output. For these reasons, implementation of dead-time is strongly recommended.

4.6 Microcontroller algorithm implementation

The flow of the final code written for the microcontroller deviates slightly from that shown in Figure 7, as the done state is omitted in favor of continuous tuning. To avoid instability, a dead zone is adopted to produce hysteresis. The algorithm changes the capacitor bank state only when the maximum switch voltage exits the dead zone. An additional flow diagram is not drawn for brevity sake.

5 Methods

A measurement setup was put together and data on the Class-E PA behavior was collected for varying degrees of load mismatch under varying levels of detuning.

The Class-E PA under test was designed for $q = 1.412$ and $d = 1$ and had $V_{dd} = 1.2V$, $m = 0.05$ and $f_0 = 1.4GHz$. The set of available capacitances in the capacitor bank was $S_{bank} = \{150fF,\ 300fF,\ 450fF,\ 600fF\}$, allowing for a maximum detuning capacitance of $1.5pF$, corresponding to a minimum q of approximately 1.172.

5.1 Measurement setup

The measurement setup consisted of the following equipment-

- Keysight DSA-Z-204A 20GHz DSO
- Keysight N2803A 30GHz active differential probe
- Rohde & Schwarz FSP40 9kHz to 40GHz spectrum analyzer
- Maury load tuner
- Lab Power supply
- ATmega328 development board
- PC

The oscilloscope was connected to the Class-E PA circuit board via the active probe, and set up to measure peak switch voltage. The measurement data was transferred to the PC where it was processed using MATLAB, and capacitor bank driving commands were sent to the USB-connected ATmega328 development board over a serial monitor.

To allow convenient detuning of the load, a PC-connected Maury load tuner together with a spectrum analyzer were used as the PA load.

A block diagram of the measurement setup is shown in Figure 10.

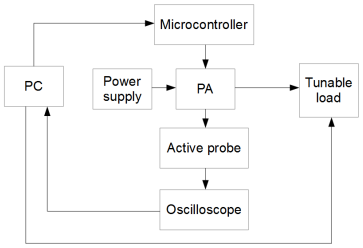

Figure 10: Block diagram of the measurement system

5.2 Tuning range

The load tuner allows a maximum load VSWR of 40; a reflection coefficient with magnitude $|\Gamma| = 0.95$. A collection of load points were chosen on the Smith chart with VSWR ranging from 0 to 40 among them. This was done to speed up the measurements, trading off the resolution of the results.

5.3 Measurement procedure

Measurements were performed by detuning the load and noting the real load power, supply voltage, supply current, reflection coefficient and switch waveform. Only the switch waveform was later used to extract the maximum switch voltage. This detuning was performed over the entire range of the load tuner.

To see the effect of the tuning system, measurements were performed at $750fF$, $1500fF$ and automatically tuned (i.e. self-healing) capacitor bank capacitance.

For the self-healing case, the load was detuned and the self-healing algorithm was run until it completes the tuning. This was done to ensure a static capacitance bank state during the recording of the measurements so the measurements would not be disturbed by a change in state. To prevent PA breakdown and possible damage, the supply V_{dd} is lowered in areas of the Smith chart where extreme maximum switch voltage behavior occurs.

5.4 Data processing

To easily compare the resulting measurement data to the theory, they were grouped into sets with similar values, these sets being plotted as points on the Smith chart. Because of the limited resolution of the results, it was decided to not interpolate the data points because of the low data density in some, and high data density in other regions (i.e. some contours have very few points and are hard to interpolate and some contours have many points and would create a contour surface rather than a line).

6 Results

The data gathered experimentally was processed and plotted as sets of data points in the Smith chart.

It should be noted that due to the time consuming nature of the measurements, the PA was measured only at select load points, as mentioned in the previous section. For this reason, the results are limited in resolution, making them slightly more difficult to interpret. Use of color gradients was employed for compactness and clarity reasons.

6.1 750fF capacitor bank capacitance

The measurement data for the PA maximum switch voltage and efficiency for $C_{bank} = 750fF$ are shown in Figure 11.

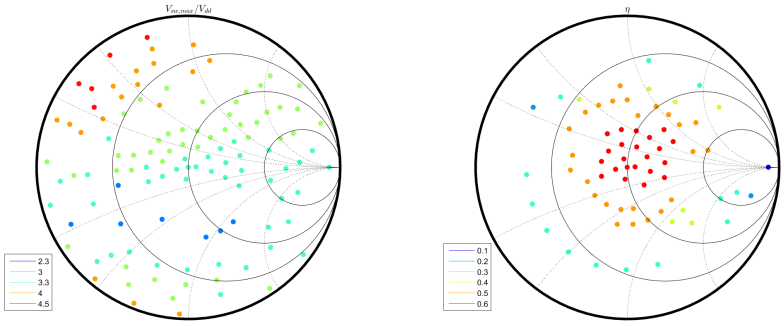

(a) $V_{sw,max}$ measurement results (b) η measurement results

Figure 11: Class-E PA contours for $C_{bank} = 750fF$

6.2 1500fF capacitor bank capacitance

The measurement data for the PA maximum switch voltage and efficiency for $C_{bank} = 1500fF$ are shown in Figure 12.

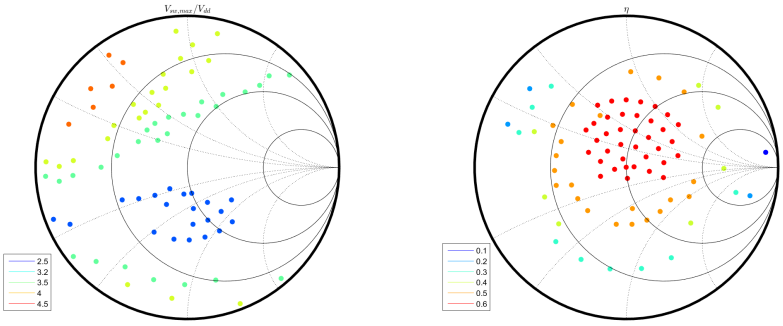

(a) $V_{sw,max}$ measurement results (b) η measurement results

Figure 12: Class-E PA measurement data for $C_{bank} = 1500fF$

It can be seen that the maximum switch voltage has reduced and the size of the zone with low peak switch voltages has increased.

6.3 Dynamic capacitor bank capacitance

Because V_{dd} was lowered in areas of the Smith chart where the PA was possibly at risk of damage, normalizing the results to $V_{dd} = 1.2V$ would present a misleading image, as the maximum switch voltage would be scaled from (the self-healed) $4V$ to a higher value for the cases where $V_{dd} < 1.2V$. This would make it seem as if the system was unable to self-heal due to the maximum switch voltage exceeding $4V$.

For this reason, instead, the points for which $V_{dd} < 1.2V$ and $C_{bank} = 1500fF$ will be shown, as these are the points where the PA cannot self-heal (i.e. if V_{dd} were raised, the maximum switch voltage would increase above the permitted limit but the system cannot add extra C_{bank} to compensate).

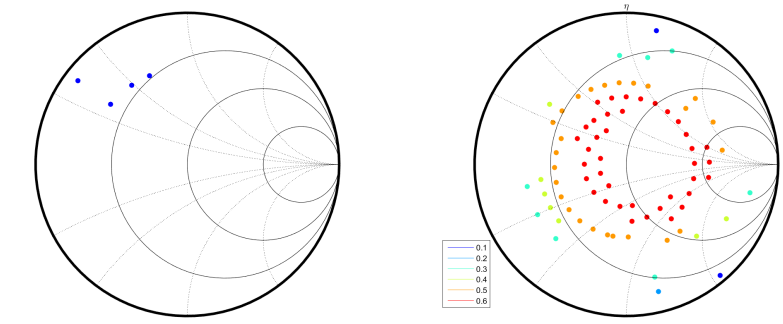

(a) Unhealable points (b) η measurement results

Figure 13: Class-E PA measurement data for the self-healing case

It is important to note that the limited number of points shown in the area where the PA cannot self-heal is due to the limited number of measurement points, not because the PA is incapable of self-healing exclusively in those points. The plots show that the PA can heal over a very large portion of the load Smith chart. Also, the area of high efficiency can be seen to have enlarged w.r.t. the static capacitor bank value measurements.

7 Discussion

The goal of this assignment was to develop a system to improve the reliability of Class-E PAs through (self-)tuning. To achieve this, the work in [1] and [2] was studied and applied. The basics of Class-E PAs were explored and laid out. After completion of the implementation of the system, experiments were performed on it and the results compared to the theoretical predictions.

7.1 Conclusions

The findings build strong confidence that Class-E PA switch voltage behavior under non-nominal load conditions can be tuned to nearly return to the nominal case by modifying the q parameter using a variable parallel switch capacitor.

The few data points breaking the general trend of the groups of other points were attributed to measurement and or recording error.

The self-healing results show improved reliability over a larger range of load mismatches, while also increasing efficiency. This shows PA parameter tuning as a viable method for self-healing Class-E PAs and presents an attractive option for future PA implementations by virtue of the efficiency benefits over other PA classes.

Additionally, the rough trend of the contours shows strong similarity to the theoretical results, albeit slightly skewed. This implies the validity of the theoretical work in [1], giving future efforts a good foundation to base other tuning methods or general Class-E research upon.

7.2 Recommendations

The measurements shown were performed after the automatic tuning system had settled. The system reaction time represents a potential problem in the protection of the PA, as the system may be too slow to properly react to a rapid load change. This requires extensive work and was therefore not studied, but may prove a fruitful area of research for future works, possibly aiding to the confidence in the reliability of future implementations.

Measurements on the effect of variations in the switch duty cycle on PA behavior were not performed. The theoretical work [1] shows a somewhat similar behavior to variation in q, so this may be another viable method of healing the PA. Using a DAC could allow for high-resolution tuning without introducing significant transmission line effects potentially associated with a large geometry capacitor bank. This presents a possibly valuable area of study for the future.

The algorithm presented for PA self-healing was designed keeping in mind only the prevention of the PA switch breakdown. It may be possible to combine this

algorithm with another that continuously adjusts the PA for optimum efficiency. Researching this might allow for increased efficiency of the self-healing PA and is therefore recommended.

A better peak detector could be designed to remove the error due to the diode forward voltage present in the system discussed in this work. A differential biased detector may be adopted to allow ideally zero-offset detection.

While q and d were discussed separately as parameters that can be varied to tune PA performance, simultaneous tuning of these parameters may provide efficiency and reliability advantages over tuning either parameter separately. More study is required to confirm or refute this.

References

[1] Ghahremani A., Annema A.-J., Nauta B. (2018). Outphasing Class-E Power Amplifiers: From Theory to Back-Off Efficiency Improvement. IEEE Journal of Solid-State Circuits, 53(5), 1374-1386. doi:10.1109/JSSC.2017.2787759

[2] Acar, M. (2011). Power amplifiers in CMOS technology : a contribution to power amplifier theory and techniques. doi:10.3990/1.9789036531382

[3] Raab, F. (1977). Idealized Operation of the Class E Tuned Power Amplifier. IEEE Transactions on Circuits and Systems, 24(12), 725-735. doi:10.1109/TCS.1977.1084296

[4] Pozar, D. (2005). Microwave engineering (3rd ed. ed.). Hoboken, NJ: J. Wiley.

Appendix A The Smith chart

The Smith chart is a commonly used graphical tool that allows intuitive solving of transmission line and impedance matching problems at radio frequencies. An empty Smith chart is shown in Figure 14.

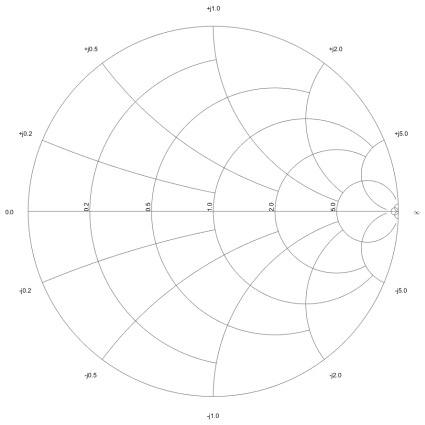

Figure 14: An empty Smith chart

A.1 Impedances on the Smith chart

The Smith chart is a polar plot of the reflection coefficient, Γ, which is given by and can be expressed as, respectively-

$$\Gamma = \frac{Z_L - Z_S}{Z_L + Z_S} \tag{12}$$

$$\Gamma = |\Gamma| e^{j\phi} \tag{13}$$

Where Z_L is the load impedance, Z_S is the system impedance and ϕ is the reflection coefficient phase.

Expressing Γ as in Equation 13 allows convenient representation in a polar plot. In this form, $|\Gamma|$ is the radius of constant $|\Gamma|$ circles centered around the origin, while ϕ, the phase of the reflection coefficient, is the angle on the Smith chart.

The Smith chart is generally drawn only for $|\Gamma| \leq 1$, as this is the maximum reflection coefficient of a passive network (for the reflected energy to be larger than the transmitted signal, the load network must be active). Additionally,

the chart is usually normalized to the system impedance, so that a single chart with normalized scale can be used to solve problems for any system impedance.

Because Equation 12 is a somewhat complex function of (normalized) load impedance, the Smith chart is somewhat complicated to interpret in terms of impedance. The mapping of the impedance plane to the Smith chart is one-to-one, however.

The reflection coefficient relates to the standing wave ratio (SWR) by-

$$|\Gamma| = \frac{SWR - 1}{SWR + 1} \tag{14}$$

Meaning SWR is also represented as the radii of circles around the origin, albeit less straightforwardly (i.e. not directly proportional to their radii).

It can be shown that constant real impedance is mapped to circles that touch on their rightmost extreme the point $\Gamma = 1$ on the Smith chart. Constant imaginary impedance similarly maps to circles with centers that lie on the line $\Gamma_{real} = 1$, also touching the $\Gamma = 1$ point [4].

Some constant resistance and reactance contours are shown in Figure 15

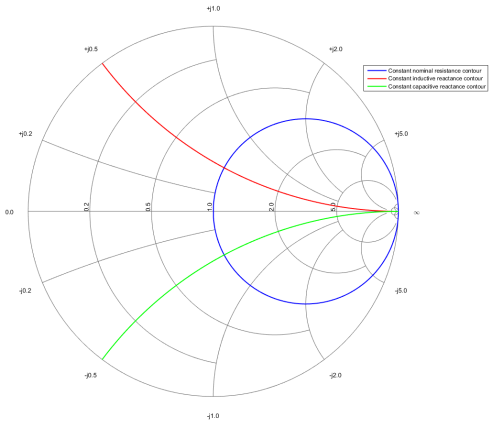

Figure 15: A Smith chart with a constant resistance (blue), constant capacitive reactance (green) and constant inductive reactance (red) contour

Because the reactive part of impedance is frequency-dependent, the Smith chart is generally used either at a single frequency, or to show the path a system follows along the Smith chart for an explicit frequency change. With regards to the Class-E PA, the Smith chart is used to represent the system at a single frequency only - the fundamental frequency of operation.

A.2 Use of the Smith chart with the Class-E PA

Because the Smith chart contains the entire complex plane, including the extremes, it is a convenient tool for graphically presenting the performance of (Class-E) PAs under any (passive) load impedance. The loss of resolution near the extremes is not an issue, as these conditions will rarely, if ever, occur in a practical situation and are thus not of significant interest.

The PA performance contours can be directly overlaid onto a Smith chart plot of the load and its variation to find the worst case PA behavior in the system.

To clearly show the trends of the PA parameters along the Smith chart, contours of constant parameters are used.

Appendix B Load Q Smith chart contours

Because the series RLC tank loaded Q represents a measure of the harmonic (i.e. non-fundamental) energy present in the load, it affects the efficiency of the PA. Additionally, significant harmonic energy emission may interfere with other equipment or violate RF regulations. For these reasons, it may be instructive to show constant Q contours on the Smith chart.

It can be shown that the additional RLC tank capacitive reactance ΔX_C required to keep Q constant for a change of tank resistance ΔR is given by-

$$\Delta X_C = \left(\frac{R^3}{2\Delta R \cdot R + \Delta R^2} + R \right) Q \tag{15}$$

Similarly, the additional RLC tank inductive reactance ΔX_L required to compensate for a change in tank resistance ΔR can be shown to be given by-

$$\Delta X_L = \left(2\Delta R + \frac{\Delta R^2}{R} \right) Q \tag{16}$$

These equations allow the generation of constant Q contours. Unfortunately, they show that these contours cannot be normalized to the nominal resistance.

To show the concept, constant Q contours on the Smith chart are presented for a tank with a nominal Q_{load} of 10 and a nominal resistance of 3.4Ω. To show the scaling effect of R, another set of contours is plotted for a nominal Q_{load} of 2. The contours are limited to $VSWR \leq 20$ to avoid clustering of the curves at the extremes of the Smith chart. It can be seen that the contours are effectively 'compressed' or 'stretched' by the scaling of the nominal Q, which is in correspondence with Equations 15 and 16.

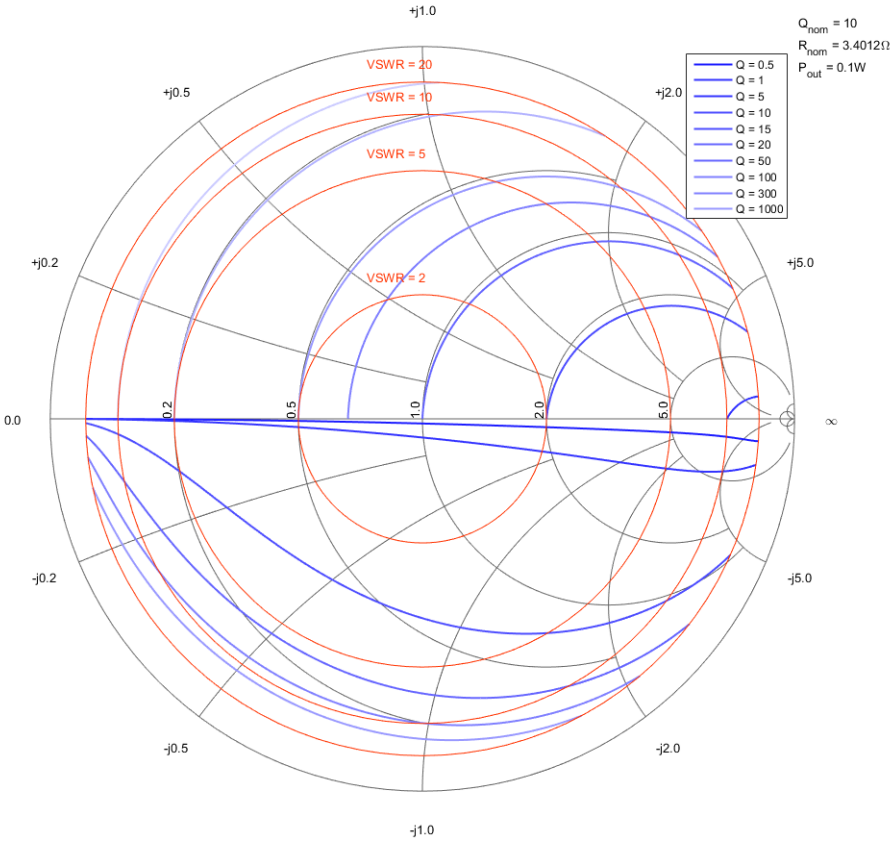

Figure 16: Constant Q contours on the Smith chart for VSWR ≤ 20 with $Q_{nom} = 10$

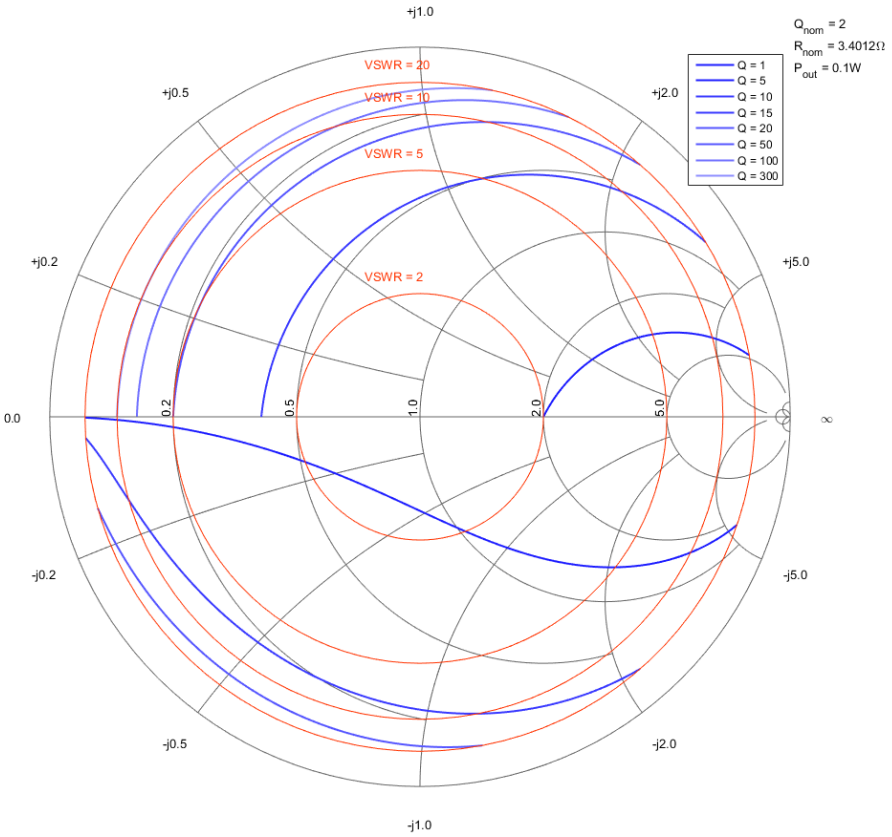

Figure 17: Constant Q contours on the Smith chart for VSWR ≤ 20 with $Q_{nom} = 2$